Antarct. Meteorite Res., **11**, 71–91, 1998

METAMORPHIC TRANSFORMATIONS OF OPAQUE MINERALS IN SOME EUCRITES

Tomoko ARAI[1], Hiroshi TAKEDA[2], Gary E. LOFGREN[3] and Masamichi MIYAMOTO[1]

[1]*Mineralogical Institute, Graduate School of Science, University of Tokyo, Hongo, Bunkyo-ku, Tokyo 113-0033*
[2]*Research Institute, Chiba Institute of Technology, Tsudanuma, Narashino 275-0016*
[3]*Johnson Space Center, NASA, Houston TX 77058, U.S.A.*

Abstract: Eucrites have undergone varying degrees of metamorphism on their parent body. We investigated mineralogical constraint on the eucrite metamorphism, especially from opaque mineralogy. Three eucrites with distinct degrees of metamorphism were studied: Y-75011,84 is the least equilibrated basaltic clast, Juvinas shows complex histories of shock and thermal metamorphism, and A-881388 is an extensively annealed and unbrecciated. Three eucrites with different metamorphic histories show distinct opaque mineralogy. In Y-75011,84, ilmenite and troilite are found crystallized in the mesostasis and opaque precipitates within pyroxenes are barely recognized. Juvinas has complicated texture, consisting of a variety of lithologies: Minute precipitates within pyroxene grains in coarse crystalline portions, larger opaque grains in granoblastic pyroxene area and recrystallized mesostases. In A-881388, during extensive prolonged annealing episode, opaque phases, such as ilmenite, troilite, and chromite are almost completely separated from silicate phases and segregated, resulting in a formation of opaque nodules. Several geothermometers, experimental results and the textural appearance of A-881388 suggest that it might have slowly cooled from near 1000–1050 °C to ≈800°C during a prolonged annealing episode. While chromite is not observed in Y-75011,84, Juvinas and A-881388 contain chromite in recrystallized mesostases and in an nodule respectively. This implies that chromite could be a metamorphic product.

1. Introduction

Eucrites are known to be among the earliest volcanic rocks on planetary surfaces and are important to understanding early planetary volcanism. They have recently drawn more attention because astronomical observations (BINZEL and XU, 1993) increase the possibility that eucrites are derived from Asteroid 4 Vesta. Most eucrites are monomict or polymict breccias, formed during cratering on the parent body (DUKE and SILVER, 1967). In rare cases, unbrecciated, crystalline eucrites have been reported, such as Ibitira (STEEL and SMITH, 1976), Caldera (BOCTOR *et al.*, 1994), and Emmaville (MASON *et al.*, 1979). Such unbrecciated eucrites are also reported among Antarctic meteorites (YANAI, 1993; TAKEDA *et al.*, 1997a; YAMAGUCHI *et al.*, 1997a). Almost all eucrites experienced various degrees of equilibration during metamorphism on its parent body (*e.g.*, TAKEDA *et al.*, 1983; TAKEDA and GRAHAM, 1991).

Eucrites are known for their simple mineralogy, consisting mainly of pyroxene and

plagioclase (*e.g.*, MASON *et al*, 1979; DUKE and SILVER, 1967) with minor silica and opaque minerals, despite a variety of secondary metamorphism. Vigorous investigations of eucrite mineralogy have turned out that most eucrites tend to have experienced complex shock and thermal metamorphism (NYQUIST *et al.*, 1997; TAKEDA and GRAHAM, 1991; TAKEDA *et al.*, 1997a,b; YAMAGUCHI *et al.*, 1994, 1995, 1996a, 1997a,b). TAKEDA and GRAHAM (1991) proposed several stages of thermal metamorphism represented by increasing degree of equilibration of eucritic pyroxenes (Type 4, 5, and 6). As such, pyroxene homogenization has been used as a measure of the equilibration of eucrites (TAKEDA *et al.*, 1983; TAKEDA and GRAHAM, 1991). In contrast, opaque mineralogy in eucrites with various extent of metamorphism have been little studied (BUNCH and KEIL, 1971; MASON *et al.*, 1979). Therefore, we have competed a systematic study of opaque minerals in eucrites, which might better constrain the metamorphism of eucrites.

Three eucrites (Y-75011,84, Juvinas, and A-881388), which range in metamorphic grade from the least equilibrated to extensively equilibrated as determined by pyroxene homogenization (TAKEDA and GRAHAM, 1991), were selected for this study. They show a distinct range in the textural appearance of the opaque minerals. Y-75011,84 is a large basaltic clast in a polymict breccia (TAKEDA *et al.*, 1983) in which the pyroxene shows extensive zoning. This sample was assigned pyroxene equilibration grade type 1 (TAKEDA and GRAHAM, 1991). Despite the largely reset ^{39}Ar-^{40}Ar system (TAKEDA *et al.*, 1994), the preservation of primary chemical zoning of pyroxene and plagioclase, and the old Sm-Nd (4.55±0.15 Ga) and Rb-Sr isochron ages (4.56±0.05 Ga) strongly support the pristinity of this clast (NYQUIST *et al.*, 1986). This indicates that Y-75011,84 is the least metamorphosed eucrite basalt known. Juvinas is a monomict breccia with several distinct textures caused by brecciation and annealing events (METZLER *et al.*, 1995; TAKEDA *et al.*, 1997a). Despite its complex textures, Juvinas evidently experienced considerable metamorphism throughout the whole sample and the degree of pyroxene homogenization is type 5 (TAKEDA and GRAHAM, 1991). Disturbance in the K-Ar age around 4.0–4.1 Ga (KANEOKA *et al.*, 1995), in contrast to the old Rb-Sr, Pb-Pb, and Sm-Nd ages of 4.50–4.56 Ga (NYQUIST *et al.*, 1986), is consistent with the brecciated nature of this sample. A-881388 is an unbrecciated, fine-grained eucrite, that has apparently suffered from extensive annealing. Its mineralogy has been studied by YANAI (1993), TAKEDA *et al.* (1997a), ARAI *et al.* (1997) and YAMAGUCHI *et al.* (1996b, 1997a). This sample has not been radiometrically dated.

Using these three eucrites that have distinctly different thermal histories, we completed mineralogical and experimental studies focused on textural and phase assemblage transformations of opaque phases that take place during metamorphism.

2. Samples and Methods

Samples of Juvinas 40E2-3, CL1, and CL5 were provided by the Muséum National d'Histoire Naturalle in Paris, and polished thin sections were prepared from chips of re'presentative lithologies (TAKEDA and YAMAGUCHI, 1991). A sample of Yamato (Y)-75011,84 and a thin section Asuka (A)-881388,51-4 were supplied by the National Institute of Polar Research.

Mineral chemistry was investigated using a JEOL 733 electron probe microanalyzer (EPMA) at the Ocean Research Institute, and a JEOL 8600 Super Probe at Geological Institute, University of Tokyo. Elemental distribution X-ray maps were obtained using the JEOL 8900 Probe at Geological Institute, University of Tokyo. Back-scattered electron images for identifying opaque phases were obtained using JEOL840A scanning electron microscope in Mineralogical Institute, University of Tokyo. Oxide phases such as ilmenite and chromite were analyzed using a beam current of 12 nA, and metal phases such as Fe metal and troilite were analyzed with a higher current of 20 nA. Troilite and Fe metal were analyzed 10–15 μm from the contact with ilmenite, taking into consideration that electron beam might excite the adjacent ilmenite.

Preliminary annealing experiments were carried out in 1 atmosphere, gas-mixing furnaces at the NASA Johnson Space Center. Natural terrestrial ilmenite, troilite, oxide mixtures with a composition of an opaque nodule in A-881388 eucrite were used as starting material for these experiments. All experiments were performed in Fe cupsules in sealed silica glass tubes to control both oxygen and sulfur fugacity: at the iron-wüstite buffer for oxygen fugacity and iron-troilite buffer for sulfur fugacity. These buffers are considered appropriate for eucrite metamorphism. The experiment duration ranged from 2 days to 2 weeks, at near solidus temperatures of 1100 °C and 1050 °C. Dr. Mike ZOLENSKY kindly provided an ilmenite sample from Kragero, Norway. Troilite #NMNH94472-2 was provided by Smithsonian Institution, Washington. Oxide mixtures were all sieved with a 125 μm mesh.

3. Results

3.1. Y-75011,84

Y-75011,84 is a basaltic clast with a subophitic texture composed mainly of pyroxene, plagioclase, and dark mesostasis (Fig. 1a). Both pyroxene and plagioclase are chemically zoned. The pyroxene zoning is extensive from relatively homogenous Mg-rich cores to Fe-rich, augite rims. Dark mesostasis is abundant (Fig. 2a) and composed of ilmenite, troilite, and silica minerals (Fig. 3a). Troilite and ilmenite exist both as discrete lath-shaped (some are irregular) grains (up to 350×200 μm and 420×160 μm, respectively), and fine-grained droplets, which occur as dusty grains in augite rims, adjacent to the mesostasis. Large, lath-shaped silica minerals (1.5×0.2 mm), crystallized intimately with ilmenite and troilite (Fig. 3b). Ilmenite and troilite are equally abundant (Table 1). Apart from dark mesostasis, other opaque phases, such as dusty opaque precipitates in pyroxenes, were not observed. The dusty augites associated with mesostases appear to be different from dusty pyroxenes generally interpreted as "clouding" phenomenon characteristic of further metamorphosed eucrites (HARLOW and KLIMENTIDIS, 1980), such as pyroxene-homogenization types 4, 5, and 6 (TAKEDA and GRAHAM, 1991) because opaque inclusions causing typical "clouding" tend to be precipitated along dislocations or exsolution lamellae of pyroxenes (HARLOW and KLIMENTIDIS, 1980). In contrast, dusty augites in this clast consist of complicated mixtures of droplets of minute ilmenite and troilite grains, together with silica minerals and fayalitic olivines to form symplectic texture (Figs. 2a, 3a), probably as a result of short-duration reheating during shock events.

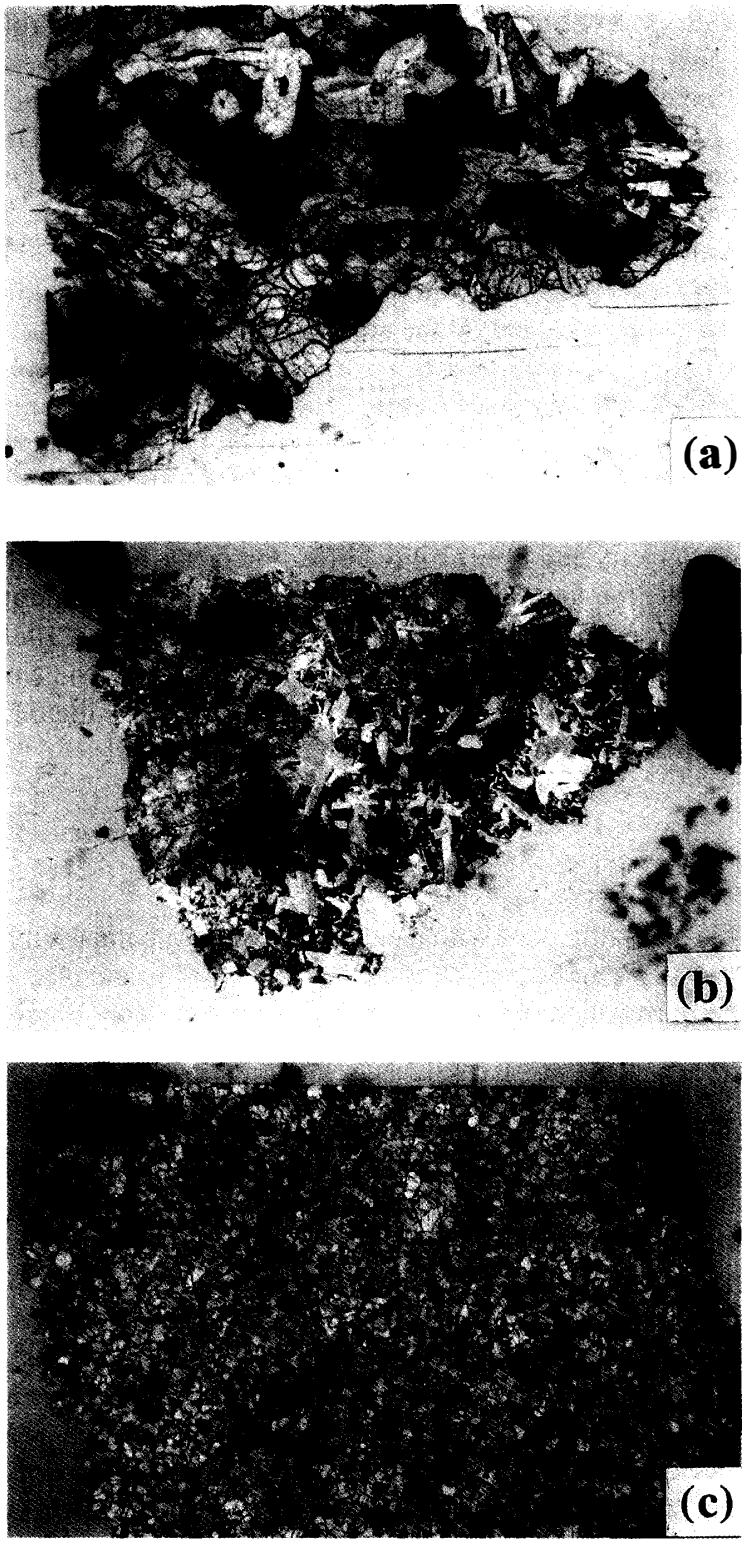

Fig. 1. Photomicrographs of whole thin sections of the eucrites studied: (a) A coarse-grained, mesostasis-rich, subophitic basaltic clast, Y-75011,84, (b) A monomict breccia with a variety of textures, Juvinas 40E2-3, and (c) A fine-grained, hornfelsic, unbrecciated eucrite A-881388,51-4. Width is 3.3 mm for all three photomicrographs.

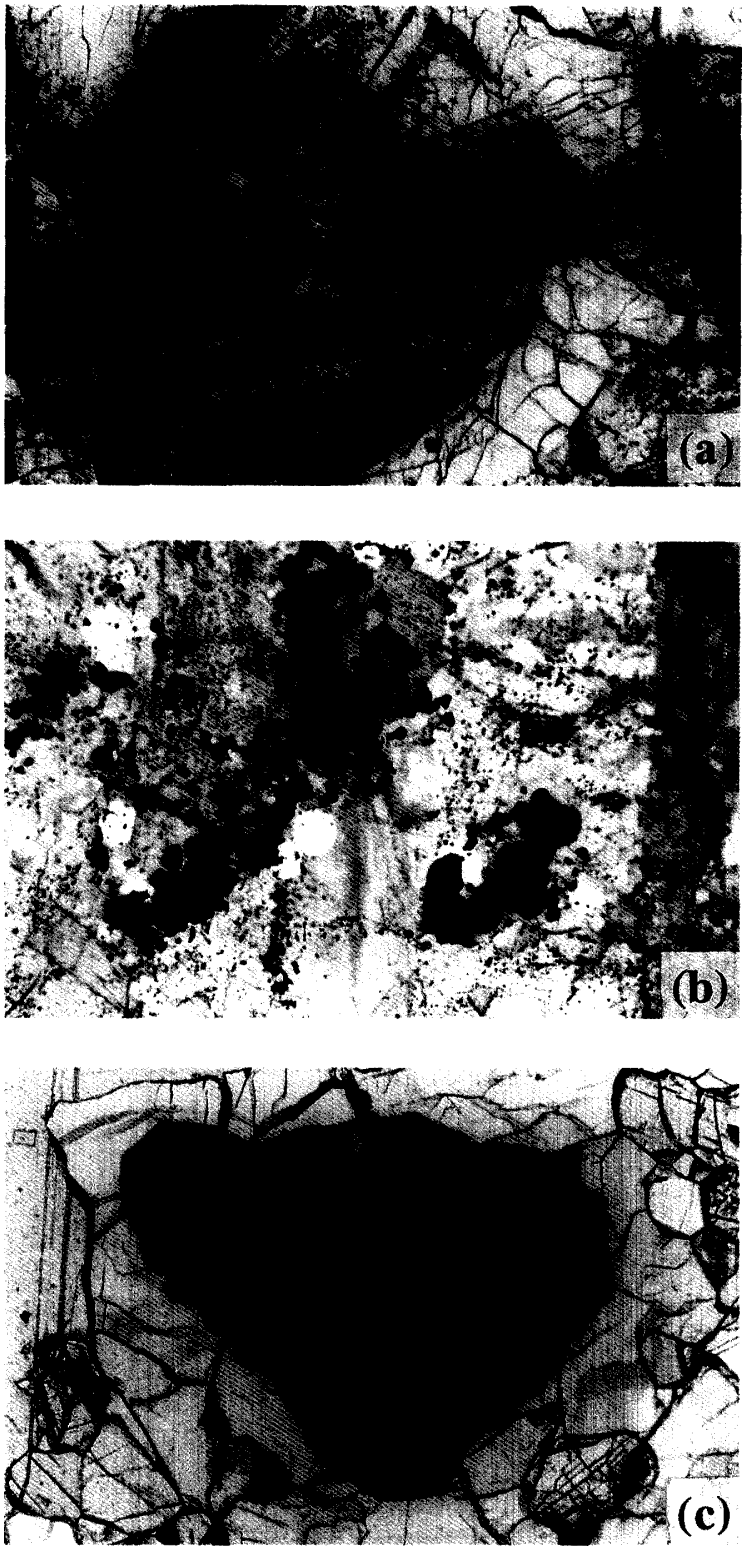

Fig. 2. Photomicrographs of areas rich in opaque minerals: (a) Ilmenite, troilite, and silica minerals in the mesostasis of Y-75011,84. In addition to the large discrete grains, troilite and ilmenite are found as minute droplets in adjacent Fe-rich augites. (b) Opaque aggregates and droplets of troilite and ilmenites in partly-recrystallized pyroxenes in Juvinas 40E2-3. (c) An opaque nodule, by far larger than surrounding silicates (plagioclase and pyroxene) in A-881388,51-4. Width is 1.3 mm for all three photomicrographs.

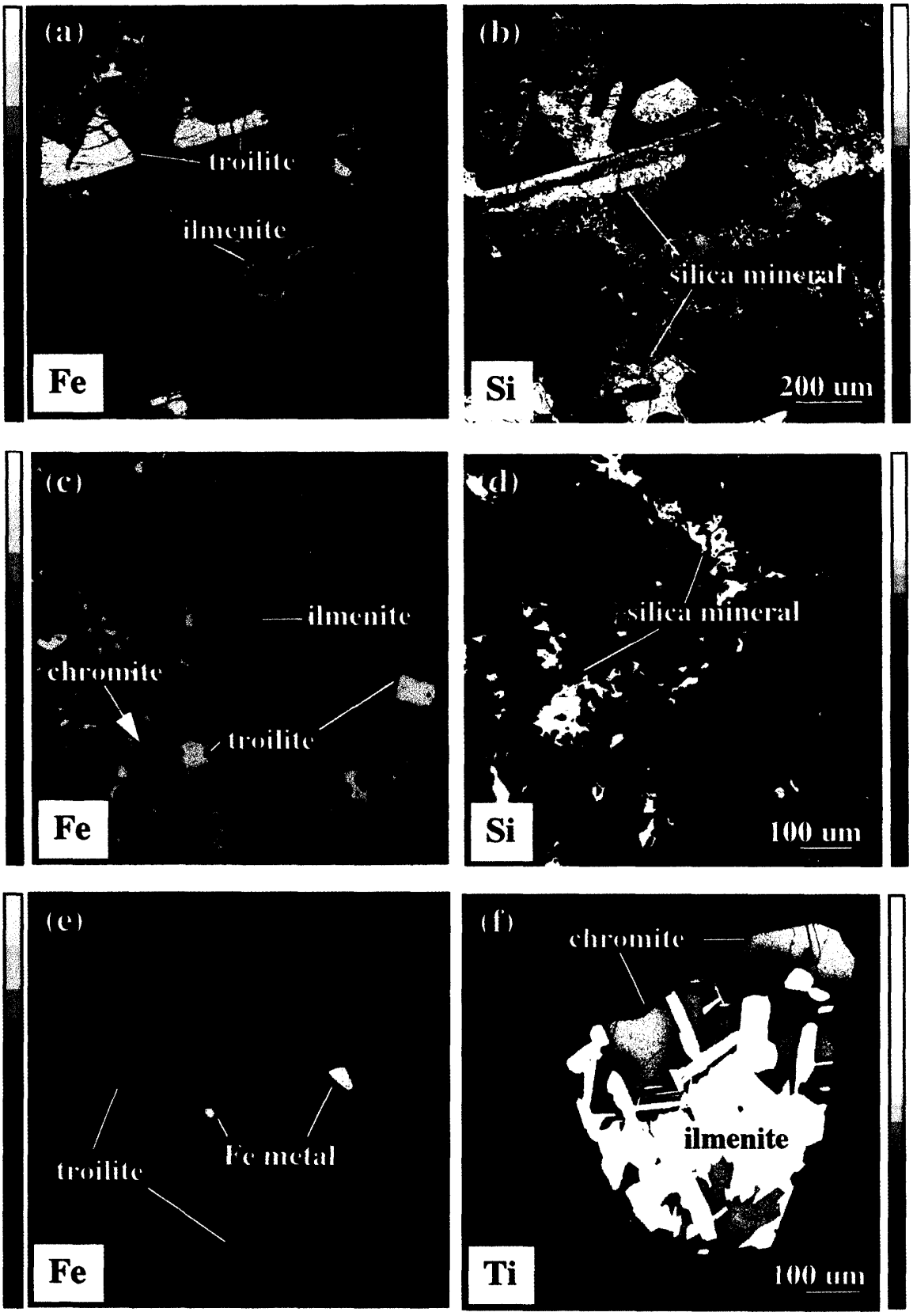
(a)
troilite
ilmenite
Fe
(b)
silica mineral
Si
200 um
(c)
ilmenite
chromite
troilite
Fe
(d)
silica mineral
Si
100 um
(e)
troilite
Fe metal
Fe
(f)
chromite
ilmenite
Ti
100 um

Fig. 3.

Table 1. Textural variations and transformations of opaque minerals, pyroxenes, silica minerals in eucrites with distinct thermal histories.

	Opaque minerals		
	Overall texture	Texture	Phases (Modes)
Y-75011,84	Subophitic, Coarse-grained	Mesostases	Ilmenite (60)+Troilite (40)
Juvinas	Locally transitional from coarse-grained to granular	Opaque precipitates in px+recrystallized mesostases	Ilm(90)+Troi (10) plus minor Chromite#
A-881388	Hipidiomorphic granular	A large nodule	Ilm (53)+Troi (12)+Fe metal (1) Plus more Chromite (34)

	Pyroxenes*	Silica minerals
Y-75011,84	Extensively zoned No opaque precipitates in px	Lath shape in mesostases with opaques
Juvinas	Exsolved pigeonite Both granoblastic clear and cloudy	Irregular shape in recrystallized mesostases
A-881388	Polygonal, no clouding Coexisting low-Ca and high-Ca px	Fine-grained ubiquitous with px and pl

* More detailed description in TAKEDA and GRAHAM (1991).
\# Chromites only in opaque assemblages are considered: precipitates in pyroxenes are not.
px: pyroxene, ilm: ilminite, troi: troilite

Fig. 3 (opposite). Elemental distribution maps (Fe, Si, and Ti) of areas rich in opaque minerals. Figures (a) and (b) correspond to the area of Fig. 2a, (c) and (d), to Fig. 2b, and (e) and (f), to Fig. 2c.
(a) Fe map of mesostases in Y-75011,84. Yellow is troilite and pink is ilmenite. Troilite and ilmenite are found both as discrete grains and as intergrowths. Fe-rich augite can also found adjacent to the mesostasis. Note that grain boundaries between ilmenite and troilite are rounded.
(b) Si map of the same area as (a). Yellow phases are lath-shaped silica minerals, which crystallized together with ilmenite and troilite. Other phases (red) are pyroxene and plagioclase.
(c) Ilmenite (pink) and troilite (yellow) crystallize together in Juvinas 40E2-3. Unlike in Y-75011,84, the troilite-ilmenite contact is linear. Micron-scale exsolution in pyroxene is remarkable. Exsolved chromites are found in ilmenite (lower left).
(d) Si map of the same portion of (c). Although silica minerals (yellow) are still closely associated with opaque phases, they are no longer lath-shaped, but are now massive.
(e) Fe map of a sub-rounded opaque nodule, consisting of an ilmenite-chromite intergrowth, troilite, and Fe metal in A-881388,51-4. Metallic Fe (yellow) grains are found at ilmenite (light purple)-titanian chromite (dark purple) contacts. Note that troilite (pink) grains crystallized along the rims of the nodule and troilites seemingly have filled in the space between the ilmenite-chromite intergrowth in a liquid state.
(f) Ti map of the opaque nodule in A-881388,51-4. Intergrowths of ilmenite (white) and titanian chromite (yellow to red) are noticeable and chromites are zoned from the rim toward the ilmenite-chromite contact.

Table 2. Chemical compositions (in wt%) of troilites and Fe metal, coexisting with ilmenites.

	Troilite					Fe metal
	Y-75011,84	Juvinas		A-881388		
Distance*	10 (μm)	10 (μm)	15 (μm)	10 (μm)	15 (μm)	10 (μm)
Co	0.1	0.1	0.1	0.1	0.0	0.2
Fe	62.6	62.6	62.3	62.2	62.6	99.8
Ni	0.0	0.0	0.0	0.0	0.0	0.0
Cr	0.0	0.0	0.0	0.0	0.0	0.1
S	36.9	36.1	36.1	36.4	36.1	0.0
Ti	0.5	0.5	0.4	0.4	0.4	1.1
Total	100.1	99.3	98.9	99.0	99.1	101.1

*A distance from the ilmenite contact.

Table 3. Chemical compositions (in wt%) of ilmenites.

	Y-75011,84	Juvinas		A-881388	
		Cr-poor	Cr-rich	Cr-poor	Cr-rich
TiO_2	53.2	53.9	53.7	53.1	52.1
Al_2O_3	0.1	0.0	0.0	0.0	0.0
FeO	44.5	44.2	44.0	43.4	43.7
MnO	1.1	0.9	1.0	0.8	0.8
MgO	0.5	1.0	1.0	1.5	1.5
Cr_2O_3	0.0	0.1	1.2	0.1	1.6
V_2O_3		0.2	0.2	0.2	0.2
Total	99.5	100.3	101.0	99.2	99.8
Cr#	0.00	0.00	0.02	0.00	0.03

Cr#=Ti/(Ti+Cr) atomic ratio.

In some mesostasis areas, troilite crystallized closely associated with ilmenite, either as an inclusion within or as an intergrowth with ilmenite (Fig. 3a). Grain boundaries in such intergrowths tend to be rounded and not euhedral. It is remarkable that troilite intergrown in ilmenite contains significant amounts of Ti. While Ti content of isolated troilite crystals is less than 0.1 wt%, those intergrown in ilmenite contain 0.27 to 0.96 wt% of Ti. Troilite which is 10 μm from the ilmenite contact includes 0.5 wt% of Ti (Table 2). Ilmenite compositions are shown in Table 3.

3.2. Juvinas

Juvinas is a breccia with a variety of lithologies caused by shock (Fig. 1b) (METZLER *et al.*, 1995; TAKEDA *et al.*, 1997b). Despite variability of the shock-related textures, the uniform chemistry of the host pigeonite in different portions of a large sample suggests that Juvinas experienced extensive metamorphism subsequent to the brecciation event. Opaque phases occur in two distinct textures: (1) Minute opaque inclusions precipitated within pyroxenes, and in veins or cracks inside pyroxenes in coarser-grained dusty areas (Fig. 4a–d) resulting in "clouding of pyroxene" (HARLOW and KLIMENTIDIS, 1980), and

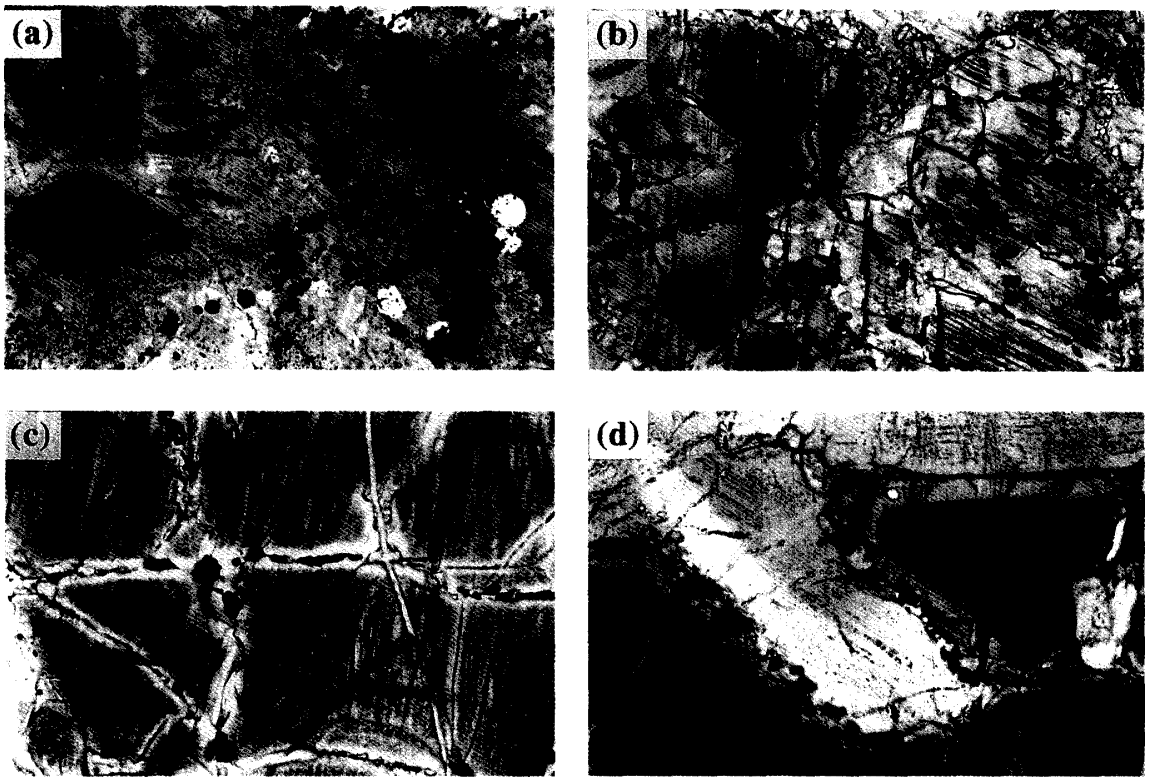

Fig. 4. Photomicrographs of clouded pyroxenes in Juvinas:
(a) A typical transition from an area with coarse-grained cloudy pyroxene to an area with opaque aggregates and opaque droplets in fine-grained clear pyroxenes in Juvinas 40E2-3. Width is 1.3 mm.
(b) Clouded pyroxene with submicron chromite crystals precipitated along exsolution planes in Juvinas 40CL1. Note that larger chromites are heterogeneously distributed probably by local coalescence of smaller chromites. Width is 650 μm.
(c) Clouded pyroxene in Juvinas 40CL5. Note that the clouded texture has been eliminated around the larger chromites due to local coalescence of minute chromites. Width is 650 μm.
(d) Grain boundaries of plagioclase and clouded pyroxene in Juvinas 40CL5. Note that larger chromites are observed along the grain boundaries and the chromite crystals have been eliminated parallel to the grain boundaries, suggesting that minute chromite in clouded pyroxenes would coalesce along the grain boundaries. Width is 650 μm.

(2) as individual grains or aggregates mixed with clear pyroxene in partly granoblastic pyroxene area (Fig. 2b). It is notable that the granular portions including opaque aggregates are consistently found adjacent to cloudy pyroxene regions with opaque precipitates (Fig. 4a).

In coarse-grained, dusty pyroxene areas, minute (micron to sub-micron) chromite grains precipitate along a plane (Fig. 4b). Among these dusty pyroxenes, some larger chromites (10–20 μm) are found locally associated with clear pyroxenes that lack minute chromite precipitates (Fig. 4b–d). Much larger chromites (10–50 μm) can be recognized in the cracks and veins within dusty pyroxenes (Fig. 4c) and along grain boundaries adjacent to pyroxene (Fig. 4d). Dusty pyroxenes are altered into clear pyroxenes near these regions. In some cracks and grain boundaries, chromite grains appear to

Table 4. Chemical compositions (in wt%) of titanian chromites in metamorphosed eucrites.

	A-881388				Juvinas
	core Ti-rich	rim Cr-rich	core Ti-rich	rim Cr-rich	
TiO_2	10.0	6.9	12.0	8.5	2.9
Al_2O_3	6.2	6.8	5.7	6.6	5.2
FeO	39.1	36.6	41.5	39.2	31.5
MnO	0.5	0.5	0.5	0.5	0.6
MgO	1.2	1.1	1.2	1.1	0.7
Cr_2O_3	41.7	48.2	38.0	43.3	57.1
V_2O_3	0.6	0.6	0.6	0.6	0.5
Total	99.3	100.8	99.4	99.9	98.5
Cr^*	0.60	0.67	0.55	0.62	0.81
Al^*	0.13	0.14	0.12	0.14	0.11
Ti^*	0.27	0.18	0.33	0.23	0.08
Cr#	0.81	0.88	0.77	0.84	0.95

Cr^*=Cr/(Cr+Al+2*Ti), Al^*=Al/(Cr+Al+2*Ti),
Ti^*=2*Ti/(Cr+Al+2*Ti), Cr#=Ti/(Ti+Cr) atomic ratios.

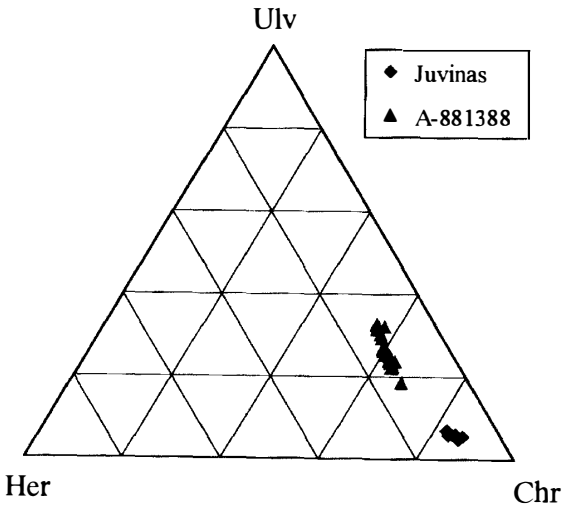

*Fig. 5. Ternary diagrams of titanian chromites in Juvinas and A-881388, represented by three components: Chr (Chromite component) = Cr/(Cr+Al+2*Ti) atomic ratio, Her (Hercynite component) = Al/(Cr+Al+2*Ti) atomic ratio, and Ulv (Ulvöspinel component) = 2*Ti/(Cr+Al+2*Ti) atomic ratio.*

partly fill the cracks, resulting in a chain of chromites, or so-called "healed-cracks" phenomenon (Fig. 4c,d) (METZLER *et al.*, 1995; HARLOW and KLIMENTIDIS, 1980).

In coarse crystalline areas, dark mesostases are found at grain boundaries of pyroxene and plagioclase (Fig. 2b). The mesostases seem to have recrystallized from the texture. The recrystallized mesostases consist of troilite and ilmenite plus minor chro-

mite (Fig. 3c) and their modal abundances are given in Table 1. Silica minerals are closely associated with these opaque phases (Fig. 3d), but do not show a lath-shape like those in Y-75011,84. They are irregularly shaped: some are massive and others are patchy. They crystallized at the boundaries between opaque phases and Ca-rich pyroxenes. Chromites are found both as small discrete grains (15×5 μm) and as exsolved grains (6 μm in width) in ilmenite (Fig. 3c). The titanian chromites are very rich in chromite component with a composition of $Chr_{82}Ulv_{7}Her_{11}$ [Chr=Cr/(Cr+Al+2*Ti), Ulv=2*Ti/(Cr+Al+2*Ti), Her=Al/(Cr+Al+2*Ti) atomic ratios] (Table 4 and Fig. 5). Troilite and ilmenite are often found co-crystallizing and their grain boundaries are sharp and linear, unlike the boundaries in Y-75011,84. Troilites adjacent to ilmenites are rich in Ti (~ 0.5 wt%) (Table 2). The Ti content increases towards the ilmenite contact. Troilite, which is 10 μm and 15 μm from the ilmenite contact, contains 0.5 and 0.4 wt% of Ti, respectively (Table 2). Figure 3c and d show one portion of an opaque aggregate (600×700 μm) in granoblastic pyroxene area which is the same portion as in Fig. 2b. Although modal abundance of troilite is lower than that in mesostasis of Y-75011,84, phase assemblages in this area are quite analogous to those of Y-75011,84 (Table 1). However, the textures of Juvinas are distinct from that of Y-75011,84 in many ways; (1) opaque droplets constituting symplectic dusty materials found in Y-75011,84 are much less abundant (Fig. 2b), (2) silica minerals apparently are massive rather than lath-shaped (Fig. 3c), (3) pyroxenes surrounding opaques are partly recrystallized to form polygonal crystals, and small chromites emerge from them, coexisting with ilmenites (Fig. 3d). These textures imply that this opaque aggregate in the coarse crystalline areas is probably recrystallized mesostasis. Minor chromite found in this opaque aggregate could originate by precipitation of chromite from nearby dusty pyroxenes. Chromium content in clear pyroxenes is one third lower than in cloudy pyroxenes (Table 5) and lower chromium concentration in clear pyroxenes most likely resulted from precipitation of chromite.

Table 5. Chemical compositions (in wt%) of pyroxenes in eucrites.

	Y-75011,84		A-881388		Juvinas+	
	Core	Rim	Low-Ca	High-Ca	Clear	Dusty
SiO_2	53.0	48.2	50.7	51.8	50.5	50.0
TiO_2	0.2	1.0	0.2	0.4	0.2	0.2
Al_2O_3	1.4	1.0	0.2	0.5	0.3	0.3
FeO	18.8	30.5	33.4	17.4	35.3	34.1
MnO	0.6	0.9	1.1	0.6	1.2	1.1
MgO	22.8	5.5	11.7	9.9	11.8	11.7
CaO	2.7	13.0	2.8	19.2	1.2	2.3
Cr_2O_3	1.0	0.0	0.1	0.2	0.1	0.3
Total	100.7	100.2	100.2	100.1	100.5	100.0
Ca^*	0.06	0.29	0.06	0.41	0.03	0.05
Fe^*	0.30	0.54	0.58	0.29	0.61	0.59
Mg^*	0.65	0.17	0.36	0.30	0.36	0.36
Cr#	0.86	0.05	0.26	0.37	0.44	0.64

+TAKEDA *et al.* (1997). Cr#=Ti/(Ti+Cr) atomic ratio.

3.3. A-881388

A-881388,51-4 is a fine-grained, unbrecciated basalt with hypidiomorphic, hornfelsic texture (Fig. 1c), similar to Emmaville and Ibitira (MASON *et al.*, 1979; STEEL and SMITH, 1976). Polygonal pyroxenes and plagioclases dominate the rock. Pyroxene grains are 0.03–0.35 mm in diameter, and consist of augite and low-Ca pyroxene. Augite lamellae ($Wo_{39}En_{31}Fs_{30}$-$Wo_{41}En_{29}Fs_{30}$) are found in host low-Ca pyroxene ($Wo_3En_{36}Fs_{61}$-$Wo_4En_{35}Fs_{61}$). Equilibrated temperature for these two pyroxenes is 800±50 °C, using two pyroxene thermometry by LINDSLEY and ANDERSON (1983). The augite exsolution is mostly around 1 μm, but locally reaches up to 10 μm. Plagioclases are 0.05–0.18 mm in diameter. Pyroxene and plagioclase are clear and free from "clouding" due to unmixed minute opaque minerals which is common in most eucrites (HARLOW and KLIMENTIDIS, 1980). Small opaque phases such as ilmenite, troilite, and less abundant chromite, are scattered both along grain boundaries of silicates, and sometimes within silicates, mostly pyroxene (Fig. 1c). An opaque nodule, that is unusually large (540×610 μm) compared with the silicate phases, is present (Fig. 1c). It has a sub-rounded triangular shape and seems to be distinct from the silicate groundmass (Fig. 2c). On one side of the thin section, a thin, brown, vesicular fusion crust (150 μm in average thickness) is observed. This fusion crust is relatively heterogeneous, incorporating partly melted pyroxenes, rounded silica minerals, and opaque crystals (ilmenite and chromite).

The opaque nodule consists of an ilmenite-chromite intergrowth with troilite and Fe-metal (Fig. 3f). The modal abundances are ilmenite 53 vol%, chromite 34 vol%, troilite 12 vol%, and Fe metal 1 vol% (Table 1). Their compositions are shown in Table 2, 3 and 4. Titanian chromites are slightly zoned from Ti-rich, Cr-poor cores ($Chr_{55}Ulv_{32}Her_{13}$) to Ti-poor, Cr-rich rim ($Chr_{62}Ulv_{25}Her_{13}$) towards the ilmenite-chro-

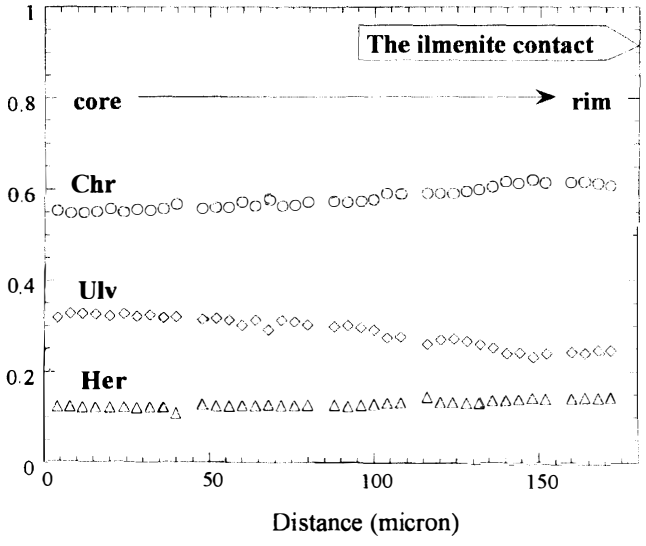

Fig. 6. Chemical zoning of titanian chromite towards the ilmenite-chromite contact in an opaque nodule of A-881388,51-4. Abbreviations of Chr, Her, and Ulv are the same as in Fig. 5. While Her stays almost constant, Chr increases and Ulv decreases toward the ilmenite-chromite contact. This trend reverses the normal zoning trend where chromites crystallize from a melt.

mite contact (Figs. 3f, 6; Table 4). However, this zoning trend is the reverse of a normal zoning trend of chromites crystallizing from the melt, where spinel composition changes from Ti-poor, Cr-rich to Ti-rich, Cr-poor (Fig. 6). Cr content in ilmenite decreases toward the boundary with chromite. Some ilmenite grains are oriented plates and others are massive. Fe metal (50 μm in diameter) is almost Ni-free and includes almost 1 wt% Ti (Table 2). Troilite crystallized along the rims of the nodule and appears to have filled in a space between silicates and chromite-ilmenite intergrowth in a liquid state. As in the case for Y-75011,84 and Juvinas, troilite contains titanium: troilite that is 10 μm from the ilmenite contact has 0.4 wt% Ti, and 15 μm from the contact has 0.35 wt% of Ti (Table1).

Smaller opaque grains (20–80 μm in diameter) scattered throughout this thin section are ilmenite and troilite. Less abundant chromites are found mainly as an intergrowth with ilmenite and some (20–30 μm in diameter) are inclusions in pyroxenes. In one opaque grain, 75×40 μm, troilite, ilmenite, and chromite coexist in the opaque nodule. Ilmenite (50 μm in diameter) with a rim of chromite is also found in the fusion crust. Silica minerals in A-881388 are as fine-grained as polygonal pyroxenes and plagioclases and are found throughout the thin section. This feature of silica minerals is quite distinct from Y-75011,84 and Juvinas.

4. Discussion

4.1. Transformation of opaque minerals and silicates during shock and thermal metamorphism

Textural variations of opaque phases in three eucrites reflect their different shock and thermal histories. In the least-equilibrated Y-75011,84, an ophitic basalt clast, opaque phases such as ilmenite and troilite are restricted to the mesostasis together with large, lath-shaped silica minerals (Figs. 2a, 3a, 3b). Ilmenite and troilite apparently crystallized at very last stage of primary crystallization. During shock and thermal metamorphism, as observed in Juvinas, chromite begins to precipitate in pyroxene producing clouding of the pyroxene. Subsequently, the chromite precipitates begin to coalesce along cracks, then move toward the pyroxene rims, and eventually to grain boundaries. Further, these chromites continue to coalesce and become associated with other opaque minerals, such as ilmenite and troilite. With such a mechanism, chromite, pre-existing ilmenite and troilite might have become segregated from silicate minerals into a nodule such as found in A-881388. Modal abundance of chromite relative to that of ilmenite + troilite is extremely high in the nodule of A-881388, compared to other two eucrites. This implies that chromite might have been produced during annealing process although a clast of Pasamonte, of which degree of equilibration is low, includes chromite (A. YAMAGUCHI, pers. commun., 1998), unlike a case of Y-75011,84. In Juvinas, opaque droplets within silicates scattered around opaque assemblages are still observed in recrystallized mesostases. In contrast, A-881388 has no opaque droplets associated with the opaque nodule, and surrounding silicates are totally clear. This also suggests complete separation of opaque phases from silicates by prolonged annealing in A-881388. The opaque nodule of A-881388 is surrounded with fine polygonal pyroxene and plagioclase

and appears to be isolated from silicates. In such extensive annealing process for A-881388, silicates present spatial constraints for separated opaque phases during recrystallization.

Fine-grained, granulitic portions with clear pyroxenes and opaque aggregates adjacent to cloudy pyroxene areas in Juvinas are comparable to the entire texture of A-881388. This implies heterogeneity of shock and thermal metamorphism in Juvinas. During the transition, chromite precipitates in pyroxene, then coalesces, and is eventually found in association with other opaque phases to form opaque nodules. The texture transitions and phases are summarized in Table 1.

For the three eucrites investigated, silica minerals display a variety of textures (Table 1; Fig. 3 b,d). While silica minerals in the mesostasis of Y-75011,84 show lath-shape or glassy, they become massive at the recrystallized mesostasis in coarse crystalline area of Juvinas. In A-881388, they are found ubiquitous and show polygonal texture as well as the pyroxenes and plagioclases. Coalescence of Fe metal and troilite and their separation from silicates are also reported as a metamorphic manifestation in chondrites (BOUTROT-DENISE *et al.*, 1997; ZANDA *et al.*, 1997). In fact, metamorphism in this case must take place at much lower temperatures and an important process in this transformation of sulfide and Fe metal is the mobilization of gaseous sulfur (LAURETTA *et al.*, 1997).

It is known that the crystal growth rate of terrestrial metamorphic rocks is controlled by the rate of diffusion between a fluid and the crystal because diffusion in metamorphic rocks is assumed to take place predominantly along grain boundaries (RIDLEY and THOMPSON, 1986). "Fluid" can accelerate solid-state crystal growth to produce hypidiomorphic granular texture. In eucrite metamorphism, fluid in the terrestrial sense is lacking, because the presence of any water or fluid on asteroid is highly unlikely. However, FeS-Fe eutectic liquid may have played a role as a fluid in eucritic metamorphism. Granular texture such as is found in A-881388 is believed to be produced by extremely slow cooling near the solidus temperature which is estimated to be 1000 to 1050°C for eucrites (STOLPER, 1977). Consistently, peak metamorphic temperature for A-881388 was estimated ~1000°C from coexisting individual pigeonite and augite (YAMAGUCHI *et al.*, 1996b). FeS-Fe eutectic liquid can be present at these temperatures because its eutectic point is 988°C (KULLERUD, 1963). Considering the coexistence of troilite and Fe metal and textural appearance of troilite in A-881388, FeS-Fe eutectic liquid might have operated as a flux during metamorphism.

4.2. Precipitation of chromite of metamorphic origin?

Eucritic basalts are known to be multiply saturated (STOLPER, 1977) and the bulk compositions of three eucrites studied here are similar to one another (Table 6), despite their different degrees of equilibration. Textures and modal abundances of opaque minerals are also distinct. BUNCH and KEIL (1971) and MASON *et al.* (1979) reported that chromite is a minor, but ubiquitous phase in eucrites and is often associated with ilmenite. A detailed description of chromites in relation to eucrite metamorphism and pyroxene equilibration, however, is lacking. According to a low-pressure, isothermal melting experiment on eucrite basalts performed by STOLPER (1977), no petrographic determination of the role of spinel in the crystallization of eucrites is yet available, though

Table 6. Bulk compositions (in wt%) of three eucrites studied.

	Y-75011#	Juvinas*	A-881388#
SiO_2	48.3	49.3	46.8
TiO_2	1.0	0.7	0.4
Al_2O_3	10.9	12.6	13.9
FeO	17.8	18.5	18.1
MnO	0.5	0.5	0.3
MgO	7.6	6.8	7.0
CaO	10.2	10.3	11.1
Na_2O	0.6	0.4	0.5
K_2O	0.1		0.0
P_2O_5	0.2		0.3
Cr_2O_3	0.4	0.3	0.2
FeS	1.1		
Total	98.4	99.2	98.5

#Catalog of Antarctic meteorites (Analysis by H. HARAMURA. YANAI and KOJIMA, 1995)
*MASON *et al.* (1979)

chromite appears almost simultaneously with silicates in the experimental crystallization sequence. Dynamic crystallization experiments on the eucrite Stannern (WALKER *et al.*, 1978) also shows that chromites crystallize with silicates above 1000°C, while ilmenite and troilite appear only below 1000°C. Despite these experimental results, no chromites are found, either as an early crystallizing phase with silicates, or as later mesostasis phase in the least equilibrated eucritic basalt, Y-75011,84. This lack of chromite has been also verified at the TEM scale in Y-75011,84 (MORI and TAKEDA, 1982). Abundant ilmenite and troilite found in mesostasis of Y-75011,84 are in accord with the result of cooling experiment by WALKER *et al.* (1978). However, chromite is found in a clast of Pasamonte, of which degree of equilibration is low (A. YAMAGUCHI, pers. Commun., 1998), unlike a case of Y-75011,84.

In contrast, apparently more metamorphosed eucrites, both Juvinas and A-881388 contain chromite, both as precipitates in pyroxenes and as a constituent of opaque assemblages (Fig. 3c,e). Modal ratio of chromite compared to other opaque minerals, such as ilmenite and troilite in A-881388, is far larger than in opaque assemblages found at recrystallized mesostases in the coarse crystalline area of Juvinas (Table 1), even though Juvinas has abundant minute chromite precipitates within pyroxenes.

Abundant, minute precipitates of chromite in cloudy pyroxene in Juvinas and larger chromite-ilmenite intergrowths with polygonal silicates in A-881388 strongly suggest that chromites found in metamorphic eucrites are derived from dusty precipitates in pyroxenes. HARLOW and KLIMENTIDIS (1980) discusses that clouding of pyroxenes might be the result of exsolution of minor components which became incompatible with a decrease in temperature and crystallized in microfractures and other nucleation sites under reducing conditions during post-brecciation metamorphism. This agrees with the fact that the clouding of pyroxene with chromite precipitates could not be observable in the least equilibrated Y-75011,84 eucrite (TAKEDA and GRAHAM, 1991). Considering that it

could not be derived from primary crystallization from the melt, chromite should be a secondary product in the process of metamorphism.

According to HARLOW and KLIMENTIDIS (1980), clouding in eucritic pyroxenes results from unmixing of ilmenite, chromite, Fe metal, as a result of reduction of Cr-, Ti-rich pyroxene during subsolidus annealing. The clouding requires a condition of T≈900°C and fO_2 of 10^{-16} to 10^{-18} during slow cooling (HARLOW and KLIMENTIDIS, 1980). Because the solubility of TiO_2 and Cr_2O_3 in pyroxene depends on FeO concentration, the presence of clouding in pyroxene strongly depends on FeO content in pyroxene: Fe/(Fe+Mg) >0.4 of pyroxene is necessary to precipitate opaques within pyroxene (HARLOW and KLIMENTIDIS, 1980). The average Fe/(Fe+Mg) = 0.6 in the A-881388 pyroxenes favors precipitation of opaque minerals in pyroxene. Lack of clouding of pyroxene in A-881388 could be due to removal of unmixed opaques during recrystallization. Chromium content of clear polygonal pyroxenes of A-881388 (Cr_2O_3 = 0.1–0.2 wt%) and in clear granoblastic pyroxenes of Juvinas (<0.1 wt%) are lower than that in dusty pyroxenes with minute chromite precipitates and much lower than that in zoned pyroxene of Y-75011,84 (Table 5). Among these three eucrites, A-881388 with the lower Cr concentration in pyroxene is likely to show higher modal abundance of chromite (Table1).

4.3. Metamorphic conditions for A-881388 and Juvinas

4.3.1. Reverse zoning in chromite in an opaque nodule of A-881388

Reverse zoning in spinel has been reported in lunar samples. Two distinct processes were suggested for its origin: (1) subsolidus reduction and (2) subsolidus equilibration. Reverse zoning caused by subsolidus reduction of chromian ulvöspinel to ilmenite, Fe metal, and sometimes aluminian-titanian chromite has been reported for Apollo14 and 16 samples (EL GORESY *et al.*, 1972, 1973; EL GORESY and RAMDOHR, 1975, 1976; HAGGERTY, 1972). EL GORESY and RAMDOHR (1977) reported that chromian ulvöspinel mantled by ilmenite or coexisting with ilmenite in Ti-rich Apollo17 mare basalts show reverse zoning. These authors noted that the ilmenites are not oriented along (111) planes of chromian ulvöspinel, as expected if they formed by subsolidus reduction of chromian ulvöspinel. EL GORESY and RAMDOHR (1977) proposed that the ilmenite rims instead formed by a reaction between chromite and a melt, or by co-precipitation from the liquid around spinel. They suggested that the reverse zoning should have been formed due to a subsolidus equilibration involving ilmenite and chromian ulvöspinel, not due to subsolidus reduction.

In the opaque nodule of A-881388, ilmenite did not crystallize as a rim of chromite: some ilmenites appear to be oriented and others are massive. The oriented platy ilmenite suggests decomposition of chromian ulvöspinel. The massive appearance may be a section parallel to the plate. Reverse zoning of chromite might have been formed by growth of ilmenite in higher-Ti-Cr complex compounds. Another possibility involves the enrichment of Cr_2O_3 in chromite and depletion in Cr_2O_3 in coexisting ilmenite toward the boundary with chromite produced primarily by subsolidus equilibration during an annealing episode. Subsolidus equilibration could have completely erased a primary crystallization zoning trend of spinel (a zoning from Ti-poor, Cr-rich core to Ti-rich, Cr-poor rim).

4.3.2 Fe metal in the opaque nodule in A-881388

Fe metal formed by reduction of FeS or FeO tends to have a lower siderophile element content (PALME *et al.*, 1988). This suggests that Ni-free Fe metal in the opaque nodule formed by reduction. Fe metal grains are found at boundaries with ilmenite-titanian chromite (Fig. 3e) suggesting that the Fe metal is a product of a reduction reaction transforming a chromian ulvöspinel to a titanian chromite + ilmenite + Fe-metal. Therefore, subsolidus reduction may result in the formation of Fe metal, and the reverse zoning of spinel, although any chromian ulvöspinel was not found in our thin section. However, YAMAGUCHI *et al.* (1997a) reported some chromian ulvöspinels, in addition to titanian chromites in a thin section A-881388,54-2. Although detailed description of the chromian ulvöspinels are not given, it is likely that the chromian ulvöspinels might be a primary spinel before the reduction reaction producing titanian chromite, ilmenite and Fe metal. Fe metal at grain boundaries of ilmenite-titanian chromite intergrowths are also common in unbrecciated eucrites, such as Ibitira (STEEL and SMITH, 1976), Caldera (BOCTOR *et al.*, 1994), and Emmaville (MASON *et al.*, 1979). However, STEEL and SMITH (1976) reported that ilmenite and titanian chromite in Ibitira show constant compositions, unlike those in the nodule in A-881388. These unbrecciated eucrites are apparently as completely metamorphosed as A-881388 (STEEL and SMITH, 1976). The reduction reaction accompanied by annealing episode appears common for such intensely metamorphosed eucrites. The presence of FeS-Fe and ilmenite-titanian chromites can constrain sulfur and oxygen fugacities of the eucrites metamorphism.

4.3.3. Equilibration temperature of metamorphosed eucrites

Equilibrium temperatures for coexisting ilmenite and titanian chromite in the presence of Fe metal was experimentally studied by KNECHT *et al.* (1977, 1979). The Cr# of exsolved chromite (Cr# [=Cr/(Cr+Ti)] = 0.95–0.96) and host ilmenite (Cr# = 0.02–0.03) in Juvinas yield equilibration temperatures far below 1000 °C. Coexisting chromite (Cr# = 0.84–0.85) and ilmenite (Cr# = 0.02–0.03) near the contact in the A-881388 opaque nodule are probably equilibrated only slightly below 1000 °C. According to thermodynamically calculated compositions of chromites (SACK and GHIORSO, 1991), chromite compositions of A-881388 may have equilibrated around 800 °C and those of Juvinas lower than 800 °C. MgO content of ilmenite coexisting with chromite in Juvinas and A-881388 (Tables 3, 4) suggests these two phases are close to equilibrium.

Troilite (FeS) and metallic Fe coexisting with ilmenite contain trace amounts of titanium, and this partitioning of titanium between these two phases has been shown experimentally to be a function of temperature (TAYLOR and WILLIAMS, 1974; TAYLOR *et al.*, 1973). TAYLOR *et al.* (1973) reported that troilite together with ilmenite in Apollo 14, Apollo15, and Apollo17 basalts contain less than 1 wt% of Ti. Compositions of troilite and Fe metal 10 μm and 15 μm from the ilmenite contact respectively are shown (Table 2). Based on the data by TAYLOR *et al.* (1973), Ti (= 0.5 wt%) in Juvinas and Ti (=0.4 wt%) in A-881388 indicate that both record equilibration temperature, about 750 °C, and 800 °C respectively.

In the unbrecciated A-881388, the equilibration temperature obtained from troilite thermometer is in accord with that obtained from low-Ca and high-Ca pyroxene pair, which is around 800 °C, and are also consistent with the coexisting ilmenite and chro-

mite which is below 1000 °C. In addition, YAMAGUCHI *et al.* (1997a) reported the peak temperature for the equilibration of A-881388 is around 1000 °C according to pyroxene thermometry of coexisting augite and pigeonite. These temperatures and the hypidiomorphic texture of A-881388 suggest that this eucrite could have cooled slowly from near the solidus temperature (1000 to 1050 °C) to ≈ 800 °C resulting in a prolonged annealing episode.

4.3.4. Preliminary experiment on the metamorphism of A-881388 and the inferred thermal history

Annealing experiments using the composition of the opaque nodule, calculated from its modal abundance were performed at 1050 °C and 1100 °C, which are high enough for FeS-Fe eutectic melts to play a role as a flux. In both experiments, assemblages of ilmenite, spinel, troilite, and Fe metal were observed. Spinels in these runs are much more Ti-rich than those found in A-881388 nodule (Fig. 7). Spinels annealed at 1050 °C for one week show slightly lower Ti content ($Chr_{30}Ulv_{63}Her_7$) than those annealed at 1100 °C for 2 days ($Chr_{26}Ulv_{70}Her_4$). It is to be noted that chromian ulvöspinels observed in the experiment at 1050 °C show almost identical compositions to those reported for another thin section of A-881388 (YAMAGUCHI *et al.*, 1997a). This implies that chromian ulvöspinels in A-881388,54-2 (YAMAGUCHI *et al.*, 1997a) could have been produced during the annealing process around 1050 °C (estimated solidus temperature of eucrites).

This result is consistent with a peak metamorphic temperature obtained from pyroxene thermometry of coexisting individual augite and pigeonite (≈ 1000 °C) (YAMAGUCHI *et al.*, 1997a). Moreover, considering ≈800 °C, an equilibrated temperature estimated from augite lamellae and host pigeonite, it is implied that prolonged annealing that A-881388 experienced probably occurred from ≈1000 °C down to ≈800 °C. Titanian chromites found in A-881388 nodule might have been produced either by reduction reaction

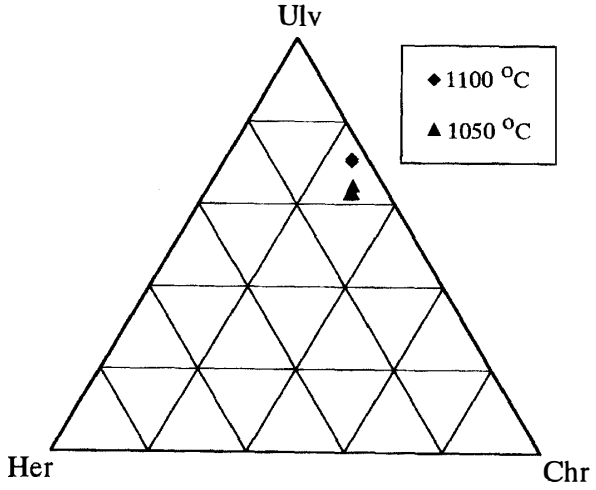

Fig. 7. Chemical compositions of chromian ulvöspinels from annealing experiments with the composition of an opaque nodule of A-881388,51-4. Abbreviations of Chr, Her, and Ulv are the same as in Fig. 5. Note that chromian ulvöspinels at 1050 °C are poorer in Ulv component in those at 1100 °C.

or by equilibration during this annealing episode.

5. Conclusions

(1) Three eucrites with different metamorphic histories show distinct opaque mineralogy. Texture and chemical compositions of opaque minerals reflect shock and thermal metamorphism eucrites experienced. In the least equilibrated eucrite, Y-75011,84, opaque minerals (ilmenite and troilite) are found as mesostasis constituents often forming symplectic textures with Fe-rich pyroxene. In Juvinas, due to complex histories of shock and annealing events, opaque minerals show diverse textural variation dependent on different lithologies: (a) minute precipitates within pyroxene grains in coarse crystalline portions, (b) larger opaque grains than the case (a) found in granoblastic pyroxene area and (c) recrystallized mesostases. In A-881388, during extensive prolonged annealing, opaque phases, such as ilmenite, troilite and chromite, are almost completely separated from silicate phases and segregated and coarsened, resulting in a formation of opaque nodules, as observed in A-881388, while silicates recrystallized to form fine-grained, granulitic texture.

(2) Studies of opaque minerals in three eucrites with different thermal histories imply that chromite could be a metamorphic product.

(3) Coexisting ilmenite-titanian chromite, and troilite-Fe metal commonly found in highly equilibrated eucrites can constrain the oxygen and sulfur fugacity for eucrite metamorphism.

(4) Several geothermometers, experimental results and the textural appearance of A-881388 suggest that it might have been slowly cooled from near 1000–1050 °C to ≈ 800 °C during a prolonged annealing episode.

Acknowledgments

The samples used in this work were provided by the National Institute of Polar Research, Japan, and the Muséum National d'Histoire Naturalle in Paris. We thank late Prof. Paul PELLAS for the separation of the Juvinas samples and Dr. A. YAMAGUCHI for the PTS preparation. This work was supported by a grant of the Ocean Research Institute, Japanese Society for Promotion of Science, Ishizaka Foundation and Tokyo Club Foundation. We are indebted to Ms. L. LEE, or her help in conducting experiments at Johnson Space Center, NASA, Mr. O. TACHIKAWA and Mr. H. YOSHIDA for their technical assistance of electron microprobe analyses at the Mineralogical Institute and the Geological Institute, University of Tokyo. We thank Drs. P. H. WARREN, J. T. WASSON, A. E. RUBIN, F. ULFF-MØLLER, M. I. PETAEV, B. ZANDA, D. S. LAURETTA, C. MANNING, A. YAMAGUCHI, J. JONES, and L. E. NYQUIST for helpful discussions.

References

ARAI, T., TAKEDA, H. and MIYAMOTO, M. (1997): Metamorphic history of a large opaque nodule in crystalline eucrite Asuka 881388. Lunar and Planetary Science XXVIII. Houston, Lunar Planet. Inst., 49–50.

BINZEL, R.P. and XU, S. (1993): Chips off of asteroid 4 Vesta: Evidence for the parent body of basaltic achon-

drite meteorites. Science, **260**, 186–191.

BOCTOR, N.Z., PALME, H., SPETTEL, B., EL GORESY, A. and MACPHERSON, G.J. (1994): Caldera: A second unbrecciated noncumulate eucrite. Meteoritics, **29**, 445.

BOUTROT-DENISE, M., ZANDA, B. and HEWINS, R. (1997): Metamorphic transformations of opaque minerals in chondrites. Workshop on Parent-Body and Nebular Modification of Chondiritic Materials. LPI Tech. Rpt. 97–02, Part 1. Houston, Lunar Planet. Inst.

BUNCH, T.T. and KEIL, K. (1971): Chromite and ilmenite in non-chondritic meteorites. Am. Mineral., **56**, 146–157.

DUKE, M.B. and SILVER, L.T. (1967): Petrology of eucrites, howardite and mesosiderites. Geochim. Cosmochim. Acta, **31**, 1637–1665.

EL GORESY, A. and RAMDOHR, P. (1975): Subsolidus reduction of lunar opaque oxides: Textures, assemblages, geochemistry, and evidence for a late-scale endogenic gaseous mixture. Proc. Lunar Planet. Sci. Conf., 6th, 729–745.

EL GORESY, A. and RAMDOHR, P. (1976): Zoning in spinels as an indicator of the crystallization histories of mare basalts. Proc. Lunar Planet. Sci. Conf., 7th, 1261–1279.

EL GORESY, A. and RAMDOHR, P. (1977): Apollo 17 TiO_2-rich basalts: Reverse spinel zoning as evidence for subsolidus equilibration of the spinel-ilmenite assemblage. Proc. Lunar Planet. Sci. Conf., 8th, 1611–1624.

EL GORESY, A., TAYLOR, L.A. and RAMDOHR, P. (1972): Fra Mauro crystalline rocks: Mineralogy, geochemistry and subsolidus reduction of the opaque minerals. Proc. Lunar Planet. Sci. Conf., 3rd, 333–349.

EL GORESY, A., RAMDOHR, P. and MEDENBACH, O. (1973): Lunar samples from Descartes site: Opaque mineralogy and geochmistry. Proc. Lunar Planet. Sci. Conf., 4th, 733–750.

HAGGERTY, S. E. (1972): Apollo 14: Subsolidus reduction and compositional variations of spinels. Proc. Lunar Planet. Sci. Conf., 3rd, 305–332.

HARLOW, G. E. and KLIMENTIDIS, R. (1980): Clouding of pyroxene and plagioclase in eucrites: Implications for post-crystallization processing. Proc. Lunar Planet. Sci. Conf., 11th, 1131–1143.

KANEOKA, I., NAGAO, K., YAMAGUCHI, A. and TAKEDA, H. (1995): ^{40}Ar-^{39}Ar analyses of Juvinas fragments. Proc. NIPR Symp. Antarct. Meteorites, **8**, 287–296.

KNECHT, B., SIMONS, B., WOERMANN, E. and EL GORESY, A. (1977): Phase relations in the system Fe-Cr-Ti-O and their application in lunar thermometry. Proc. Lunar Planet. Sci. Conf., 8th, 2125–2135.

KNECHT, B., WOERMANN, E. and EL GORESY, A. (1979): Element distributions among spinel and ilmenite phases in the system FeO-Cr_2O_3-TiO_2, FeO-Al_2O_3-TiO_2 and FeO-MgO-TiO_2. Lunar and Planetary Science X. Houston, Lunar Planet. Inst., 760–672.

KULLERUD, G. (1963): The Fe-Ni-S system. Carnegie Inst. Washington Year Book, **62**, 175–189.

LAURETTA, D.S., LODDERS, K., FEGLEY, B., Jr. and KREMSER, D.T. (1997): The origin of sulfide-rimmed metal grains in ordinary chondrites. submitted to Earth Planet. Sci. Lett.

LINDSLEY, D.H. and ANDERSON, D.J. (1983): A two-pyroxene thermometer. Proc. Lunar and Planetary Science Conf., 13th, Pt. 2, A887–A906 (J. Geophys. Res., **87** Suppl.)

MASON, B., JAROSEWICH, E. and NELEN, J.A. (1979): The pyroxene-plagioclase achondrites. Smithson. Contrib. Earth Sci., **22**, 27–45.

METZLER, K., BOBE, K.-D., PALME, H., SPETTEL, B. and STÖFFLER, D. (1995): Thermal and impact metamorphism of the HED parent body. Planet. Space Sci., **43**, 499–525.

MORI, H. and TAKEDA, H. (1982): Analytical electron microscopic studies of pigeonites in eucrites. Papers Presented to the 7th Symposium on Antarctic Meteorites, Feb. 19–20, 1982. Tokyo, Natl Inst. Polar Res., 26–28.

NYQUIST, L.E., TAKEDA, H., BANSAL, B.M., SHIH, C.-Y., WIESMANN, H. and WOODEN, J. (1986): Rb-Sr and Sm-Nd internal isochron ages of a subohitic basalt clast and matrix sample from the Y-75011 eucrite. J. Geophys. Res., **91**(B8), 8137–8150.

NYQUIST, L.E., BOGARD, D., TAKEDA, H., BANSAL, B.M., WIESMANN, H. and SHIH, C.-Y. (1997): Crystallization, recrystallization, and impact-metamorphic ages of eucrites Y792510 and Y791186. Geochim. Cosmochim. Acta, **61**, 2119–2138.

PALME, H., WLOTZKA, F., SPETTEL, B., DREIBUS, G. and WEBER, H. (1988): Camel Donga: A eucrite with high metal content. Meteoritics, **23**, 49–57.

RIDLEY, J. and THOMPSON, A.B. (1986) The role of mineral kinetics in the development of metamorphic microtextures. Fluid-rock Interactions during Metamorphism, ed. By J.V. WALTHER and B.J. WOOD. New York, Springer, 154–193.

SACK, R.O. and GHIORSO, M.S. (1991): Chromian spinels as petrogenetic indicators: Thermodynamics and petrological applications. Am. Mineral., **76**, 827–847.

STEEL, I. M. and SMITH, J.V. (1976): Mineralgy of the Ibitira eucrite and comparison with other eucrites and lunar samples. Earth Planet. Sci. Lett., **33**, 67–78.

STOLPER, E. (1977): Experimental petrology of eucritic meteorites. Geochim. Cosmochim. Acta, **41**, 587–611.

TAYLOR, L.A. and WILLIAMS, K.L. (1974): Formational history of lunar rocks applications of experimental geochemistry of the opaque minerals. Proc. Lunar Planet. Sci. Conf., 5th, 585–596.

TAYLOR, L.A., MCCALLISTER, R.H. and SARDI, O. (1973): Cooling histories of lunar rocks based on opaque mineral geothermometers. Proc. Lunar Planet. Sci. Conf., 4th, 819–828.

TAKEDA, H. and GRAHAM, A.L. (1991): Degree of equilibration of eucrite pyroxenes and thermal metamorphism of the earliest planetary crust. Meteoritics, **26**, 129–134.

TAKEDA, H. and YAMAGUCHI, A. (1991): Recrystallization and shock textures of old and new samples of Juvinas in relation to its thermal history. Meteoritics, **26**, 400.

TAKEDA, H., WOODEN, J.L., MORI, H., DELANEY, J.S., PRINTZ, M. and NYQUIST, L.E. (1983): Comparison of Yamato and Victoria land polymict eucrites: A view from mineralogical and isotopic studies. Proc. Lunar Planet. Sci. Conf., 14th, Pt.1, B245–B256 (J. Geophys. Res., **88** Suppl.).

TAKEDA, H., MORI, H. and BOGARD, D. D. (1994): Mineralogical and ^{39}Ar-^{40}Ar age of an old pristine basalt: Thermal history of the HED parent body. Earth Planet. Sci. Lett., **122**, 183–194.

TAKEDA, H., ISHI, T. ARAI, T. and MIYAMOTO, M. (1997a): Mineralogy of the Asuka 87 and 88 eucrites and crustal evolution of the HED parent body. Antarct. Meteorite Res., **10**, 401–413.

TAKEDA, H., YAMAGUCHI, A., KANEOKA, I. and NAGAO, K. (1997b): Shock and recrystallization history of Juvinas in relation to the crustal evolution of a Vesta-like body. submitted to Meteorit. Planet. Sci.

WALKER, D., POWELL, M.A., LOFGREN, G.E. and HAYS, J.F. (1978): Dynamic crystallization of a eucrite basalt. Lunar Planet. Sci. Conf., 9th, 1369–1391.

YAMAGUCHI, A., TAKEDA, H., BOGARD, D.D. and GARRISON, D.H. (1994): Textural variation and imapct history of the Millbillillie eucrite. Meteoritics, **29**, 237–245.

YAMAGUCHI, A., TAYLOR, J.G. and KEIL, K. (1995): Mineralogical study of some Antarctic monomict eucrites including Yamato 74356- A unique rock containing recrystallized clastic matrix. Proc. NIPR Symp. Antarct. Meteorites, **8**, 167–184.

YAMAGUCHI, A., TAYLOR, J.G. and KEIL, K. (1996a): Global crustal metamorphism of the eucrite parent body. Icarus, **124**, 97–112.

YAMAGUCHI, A., TAYLOR, J.G. and KEIL, K. (1996b): Three unbrecciated eucrites: Global metamorphism on the eucrite parent body. Lunar and Planetary Science XXVII. Houston, Lunar Planet. Inst., 1469–1470.

YAMAGUCHI, A., TAYLOR, J.G. and KEIL, K. (1997a): Shock and thermal history of equilibrated eucrites from Antarctica. Antarct. Meteorite Res., **10**, 415–436.

YAMAGUCHI, A., TAYLOR, J.G. and KEIL, K. (1997b): Metamorphic history of the eucrite crust of 4 Vesta. J. Geophys. Res, **102**, 13381–13386.

YANAI, K. (1993): The Asuka-87 and Asuka-88 collections of Antarctic meteorties: Preliminary examination with brief descriptions of some typical and unique-unusual specimens. Proc. NIPR Symp. Antarct. Meteorites, **6**, 148–170.

YANAI, K. and KOJIMA, H. (1995): Catalog of Antarctic Meteorites. Tokyo, Natl Inst. Polar Res., 230 p.

ZANDA, B., YU, Y., BOUTROT-DENISE, M. and HEWINS, R. (1997): The history of metal and sulfides in chondrite. Workshop on Parent-Body and Nebular Modification of Chondiritic Materials. LPI Tech. Rpt. 97-02, Part 1. Houston, Lunar Planet. Inst., 68.

(Received October 13, 1997; Revised manuscript accepted January 29, 1998)